

Development of planar CT system for multi-layer PCB inspection

Seung Ho Kim^a, Hanbean Youn^a, Soohwa Kam^a, Eunpyeong Park^a, Ho Kyung Kim^{a,b*}

^aSchool of Mechanical Engineering, Pusan National University, Busan, South Korea

^bCenter for Advanced Medical Engineering Research, Pusan National University, Busan, South Korea

*Corresponding author: hokyung@pusan.ac.kr

1. Introduction

Non-destructive testing (NDT) is essential for manufacturing reliability. It is impossible to inspect inner defects in a multi-layer printed circuit board (PCB) using optical testing. Alternatively, X-ray defect inspection apparatus can be used in the production line to inspect the PCB. However, a simple X-ray radiography cannot discriminate defects from the multi-layer PCBs because the layers of them overlays the defects. To complement this issue, computed tomography (CT) technology is applied to the NDT system which can offer 3-dimensional information of object. However, CT requires hundreds of projection images to examine a single PCB, hence real-time inspection is nearly impossible.

In this study, we develop a planar computed tomography (pCT) system appropriate for the multi-layer PCB inspection. For the image reconstruction of planar cross-section images, we use the digital tomosynthesis (DTS) concept in association with the limited angle scanning.

2. Material and Methods

2.1 The pCT system

The pCT is an intermediate concept between 2-d radiography and CT. It acquires projection images in limited angular ranges, and reconstructs 3-d-like tomographic slices in short acquisition and reconstruction time. Although the depth resolution of the conventional CT approach is limited by lack of projection data obtained from the limited angular range, it is reported that the DTS concept can provide sufficient depth resolution. The pCT system is composed of X-ray source, detector and rotation stage as the same as the CT systems.

The image acquisition concept of the pCT is basically follows CT systems. However, the image acquisition geometry of the pCT systems can be diverse; the iso-centric motion (fixed detector with iso-centrally moving source), fully circular motion, and linear motion. In this study, we choose the circular motion.

For the image reconstruction, we use the GPU accelerated filtered backprojection(FBP) DTS method [1, 2]. Unlike the convention FBP method used in CT, the DTS algorithm requires additional filters such as spectral apodization filter and slice thickness filter. The spectral apodization filter is designed to reduce the high frequency noise, which is amplified due to the ramp filter.

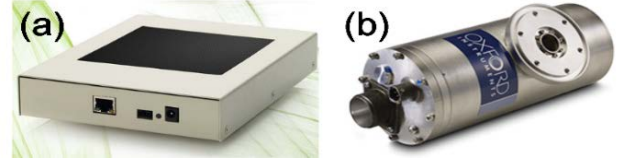


Fig. 1. (a) Shad-o-Box 1548 HS CMOS detector Teledyne Dalsa Inc, USA), (b) Tungsten target micro focal spot x-ray tube Apogee (Oxford Instruments Inc, USA)

The typical apodization filter is the Hann filter, which is given by

$$H_{SA} = \frac{1}{2} \left[1 + \cos \left(\frac{\pi \mu}{k_{SA}} \right) \right], \quad (1)$$

where μ is the spatial frequency and k_{SA} denotes the bandwidth of the Hann filter, which can be adjusted by multiplication of Nyquist frequency. The slice thickness filter is designed to avoid the noise aliasing along the vertical direction [1, 3]. The slice thickness filter used in this study is also the Hann filter and it is given by

$$H_{ST} = \frac{1}{2} \left[1 + \cos \left(\frac{\pi \omega}{k_{ST}} \right) \right], \quad (2)$$

where the ω is the Fourier conjugate of the z-direction, and k_{ST} denotes the bandwidth of slice thickness filter. The k_{ST} depends on the total scan angle of the system such as

$$k_{ST} = u_N \times \tan \left(\frac{\beta_{scan}}{2} \right), \quad (3)$$

where β_{scan} is the total scan angle and u_N is the Nyquist frequency of the u direction. Algorithm

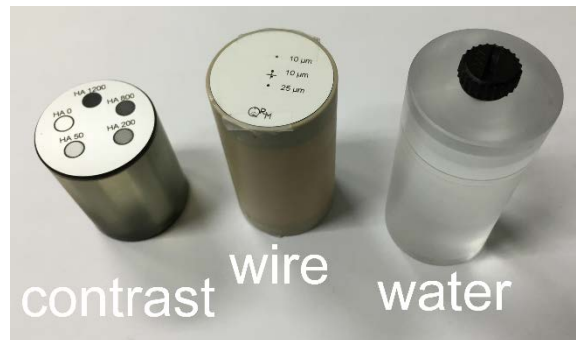


Fig. 2. QRM phantoms(cylinder, wire, and water)

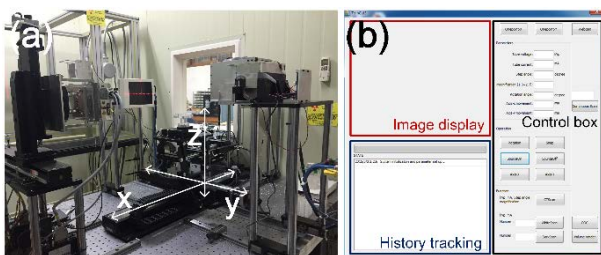


Fig. 3. (a) DTS system (b) GUI design

acceleration using the GPU is implemented by using CUDA (compute unified device architecture, Nvidia, USA). We install the CUDA-enabled GPU (Tesla k20c), which have 706 MHz cores and 5120 MB memories.

2.2 System specification

The flat-panel detector (FPD), which is fabricated by a complementary metal-oxide-semiconductor (CMOS) process, is used as shown in Fig. 1(a). The FPD has small 0.099 mm-sized pixels arranged in 1032×1548 format. And it has the maximum frame rate 20 frames per second (fps). The CMOS FPD has some advantages, such as high frame rate, low image lag, low readout noise, small pixel size, high fill factor. Since the typical DTS systems used tens of projections, therefore, we expect that we can implement the semi-real-time inspection capability with GPU-accelerated image reconstruction.

Tungsten target micro focal spot x-ray source, which has maximum anode current of 1 mA and maximum anode voltage of 50 kVp, and focal spot size of 35 μm , is used as shown in Fig. 1(b).

For the flexibility in image acquisition geometries, we use automated linear motion guides along x-, y-, z-direction. The maximum travel range along each direction is determined to be 600, 300, and 75 mm, respectively. The overall control sequences are integrated on the computer-controlled software.

2.3 Performance characterization

To characterize the performance of the pCT system, we use the Fourier metrics, such as modulation-transfer function (MTF) [4], noise-power-spectrum (NPS) [5], and detective-quantum efficiency (DQE) [6] for the FPD evaluation, and MTF, NPS, and NEQ for system evaluation. Experimental conditions are summarized in table I.

The measurement of system performance, we use quantitative phantoms, such as the water cylinder, and the wire phantom as shown in Fig. 2. The MTF of pCT system can be calculated by using the slanted slit method by using the wire phantom. We calculate fine-sampled line-spread function from the volume image of wire phantom. Then the Hankel transform is applied. The NPS is calculated by using the water phantom. Considering that the shift variant characteristics of the NPS of the pCT system, we evaluate the regions of interest (ROIs) at the radially

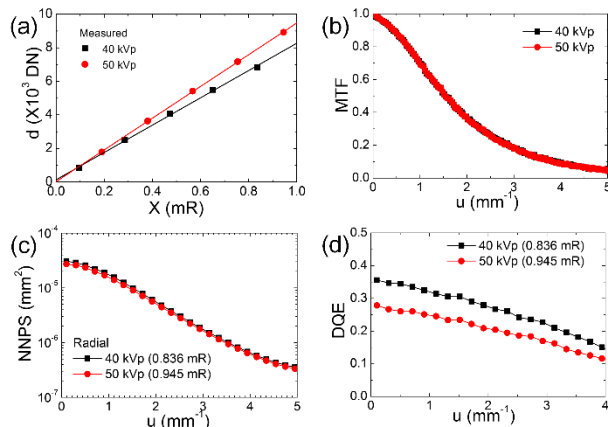


Fig. 4. Imaging characteristics of the Shad-o-Box HS CMOS detector configuration : (a) Characteristic curve (b) MTF (c) NNPS (d) DQE

Table I: Detector evaluated performance conditions

Voltage	40 kVp	50 kVp
Additional filter	3 mmAl	3 mmAl
Source to detector distance	550 mm	550 mm
Frame rate	200 ms	200 ms
Current	0.9 mA	0.5 mA
Half value layer	1.727 mmAl	2.259 mmAl

equivalent position. Then, the 3-d Fourier transform is applied.

3. Preliminary results

Figure 3(a) show the pCT system developed in this study. To realize the circular motion, we install the rotational stage between the x-ray source and detector. The rotational stage can be moved along the x-, y-, and z-directions by the linear motion controls. For a stable operation, air-cooling system is equipped on the x-ray tube and geometrical guides using the laser is applied. All the operations are conducted by using the integrated graphical user interface depicted in Fig. 3(b). As shown in Fig. 3(b), the image display section, history tracking section, and the control sections are prepared. .

As preliminary results of the system characterization, the performance results of FPD are shown in Fig. 4. The characteristic curve of the detector is very linear down to the very low exposure levels. We find out the 10 % of MTF reaches about 4 lp/mm. We expect a better MTF performance where we provide a magnification. As shown in Fig. 4(d), the DQE performance of 40 kVp is higher than the 50 kVp because we use a thinner phosphor screen in the FPD to acquire the high resolution. Although the DQE performance at the lower frequency is not high enough compared with the typical radiography detectors, the higher frequency region, however, the DQE seems to be acceptable for PCB inspection.

4. Further study

In this study, we focused on the development procedure and performance characterization of the pCT system for the PCB inspection. The 3-d Fourier characteristics and more quantitative performance, such as contrast, uniformity, depth resolution will be presented. The cross-sectional images of multi-layer PCBs will also be demonstrated.

ACKNOWLEDGMENTS

This work was supported by the National Research Foundation of Korea (NRF) grant funded by the Korea government (MSIP) (No. 2013M2A2A9046313).

REFERENCES

- [1] H. Youn, J. S. Kim, M. K. Cho, S. Y. Jang, W. Y. Song, and H. K. Kim, Optimizing imaging conditions in digital tomosynthesis for image-guided radiation therapy, *Korean J. Med. Phys.*, Vol. 21(3), pp. 281–290, 2010.
- [2] J. T. Dobbins III, and D. J. Godfrey, Digital x-ray tomosynthesis: current state of the art and clinical potential, *Phys. Med. Biol.*, Vol. 48(19), pp. R65, 2003.
- [3] G. Lauritsch, and W. H. Härer, Theoretical framework for filtered back projection in tomosynthesis, *Proc. SPIE*, Vol. 3338, pp. 1127–1137, 1998.
- [4] H. Fujita, D. Y. Tsai, T. Itoh, J. Morishita, K. Ueda, A. Ohtsuka, A simple method for determining the modulation transfer function in digital radiography, *IEEE Trans. Med. Imaging.*, Vol. 11(1), pp. 34–39, 1992.
- [5] M. B. Williams, P. A. Mangiafico, and P. U. Simoni, Noise power spectra of images from digital mammography detectors, *Med. phys.*, Vol. 26(7), pp. 1279–1293, 1999.
- [6] M. K. Cho, H. K. Kim, T. Graeve, S. Yun, C. H. Lim, D. H. Cho, and J. M. Kim, Measurements of x-ray imaging performance of granular phosphors with direct-coupled cmos sensors, *IEEE Trans. Nucl. Sci.*, Vol. 55(3), pp. 1338–1343, 2008.